Slow collisions of H^- and D^- with Na and K

Yicheng Wang, R. L. Champion, and L. D. Doverspike
Department of Physics, College of William and Mary, Williamsburg, Virginia 23185
(Received 22 September 1986)

Relative cross sections for charge transfer and electron detachment in collisions of H^- and D^- ions with Na and K atoms have been measured in the energy range from 2 to 300 eV. Measurements of the differential elastic cross sections for collisions of H^- with Na are also reported for energies around 10 eV. A two-state perturbed-stationary-state calculation has been performed and compared with the experimental results and a previous calculation.

I. INTRODUCTION

Slow collisions of hydrogen negative ions with alkali-metal atoms have recently been the focus of considerable attention since it is known that the presence of cesium vapor in an H^- ion source, which employs a plasma discharge, can dramatically enhance the efficiency of H^- production.[1–6] Theoretically, Karo *et al.*[3] performed multiconfiguration self-consistent-field (MCSCF) calculations for the potential curves of ground states of several alkali hydrides and their corresponding negative molecular ions. Olson and Liu[4] calculated configuration-interaction (CI) potential curves for the low-lying states of NaH and NaH^- (see Fig. 1), and based on their CI potential curves and a two-state perturbed-stationary-state (PSS) approximation, they estimated the charge transfer as well as the electron-detachment cross sections for $H^- + Na$ for energies below 400 eV. They also obtained the cross sections for $H^- + K$, Rb, and Cs by scaling the results for $H^- + Na$ to account for the different dipole polarizabilities and electron affinities of the alkali-metal atoms. Experimentally, Meyer[5] measured total electron-loss cross sections for H^- $(D^-) + Cs$ in the energy range from 150 eV to 2 keV utilizing beam attenuation methods. Tuan and Esaulov[6] obtained differential energy-loss spectra of scattered H atoms for $H^- + Na$ with a time-of-flight apparatus and, based on the spectra, estimated the ratios of the charge transfer to the electron detachment cross sections for energies ranging from 100 to 500 eV.

For energies above approximately 500 eV, there have been a number of experiments in which the "equilibrium fractions" for collisions of hydrogen (and deuterium) atoms and ions with alkali-metal vapors have been measured. A review of those measurements may be found in Schlachter *et al.*[7]

Nevertheless, the theoretical and experimental results reported so far have not been sufficient to elucidate the nature of the electron-loss mechanism for slow collisions of hydrogen negative ions with alkali-metal atoms. First of all, theoretical discrepancies still appear to exist: Olson and Liu[4] state that there is no apparent crossing of the ionic $X\,^2\Sigma$ state into the $X\,^1\Sigma$ continuum, while the calculations by Karo *et al.*[3] indicate that such a crossing occurs in the region $R \approx 3a_0$. Olson and Liu[4] suggest that the principal mechanism for electron loss is due to the long-range coupling between the $X\,^2\Sigma$ and $A\,^2\Sigma$ states of NaH^-; they predict the threshold energy for electron loss to be around 15 eV with charge transfer dominating electron detachment for all energies below 400 eV. The potential calculations by Karo *et al.*,[3] on the other hand, imply that detachment due to the coupling near the crossing between the $X\,^2\Sigma$ and $X\,^1\Sigma$ states is not negligible and has an energetic threshold close to zero. The experimental results tend to support the supposedly less accurate MCSCF potential curves: the differential energy-loss spectra of scattered H for $H^- + Na$ measured by Tuan and Esaulov[6] show that the electron detachment is comparable in magnitude to the charge transfer, which leads them to conclude that detachment due to the coupling between the ionic $X\,^2\Sigma$ state and the $X\,^1\Sigma$ continuum is one of the main causes of the discrepancy between theory and experiment. Furthermore, the total electron-loss cross section of $H^- + Cs$ measured by Meyer[5] is two to three times larger and, in addition, displays a much weaker energy dependence than that predicted by Olson and Liu. Finally, no direct cross-section measurements of charge transfer

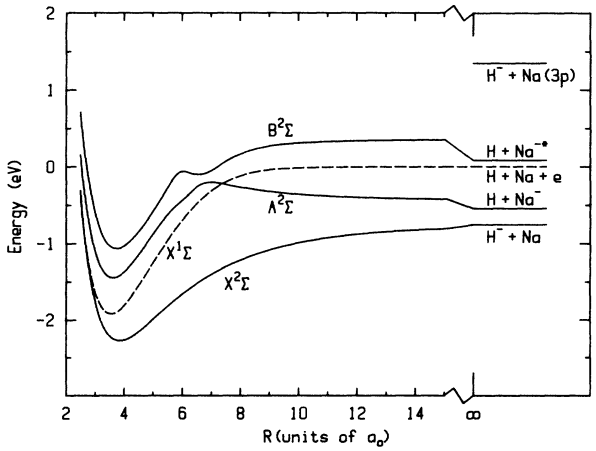

FIG. 1. Low-lying molecular states of NaH^- (solid lines) and ground state of NaH; from Ref. 4.

$\sigma_{CT}(E)$ or electron detachment $\sigma_e(E)$ for collisions of hydrogen negative ions with alkali-metal atoms have been reported in the low-energy regime.

In this paper, we report the measured cross sections of charge transfer and electron detachment for $H^-(D^-) + Na$ and K for collision energies ranging from 2 to 300 eV. We also present the measured differential elastic cross sections for $H^- + Na$ for energies around 10 eV.

II. EXPERIMENTAL APPARATUS AND METHODS

A. Crossed-beam apparatus

A schematic diagram which illustrates the main features of the apparatus used in the total-cross-section measurements is given in Fig. 2. H^- and D^- ion beams are produced in a discharge source similar to that used in this laboratory for studies of collisions of anions with gaseous targets.[8,9] After extraction, the H^- and D^- ions are focused electrostatically and mass-selected with a Wien filter; the ion beam is then focused into the collision region.

The collision region is within a one-sixth section of a 127° cylindrical electrostatic energy analyzer. The voltage across the two curved plates of the analyzer allows the ion beam to pass resonantly through the analyzer section. The primary ion beam transmitted through the analyzer section is monitored with a Faraday-cup—electrometer combination. The grid above the cup serves to determine the energy and energy spread of the ion beam, which is less than 5% of the transmission energy for all measurements reported here. It also serves to suppress any secondary electrons produced in collisions of the ion beam with the Faraday cup. The ion beam intersects, midway of its path inside the analyzer, with a neutral target beam. The electric field maintained across the analyzer is used to extract the slow anions and electrons produced in the collision region through a grid on the inner plate. The extracted anions and electrons are then focused with an einzel lens, separated by a magnetic field and detected with conventional particle multipliers.

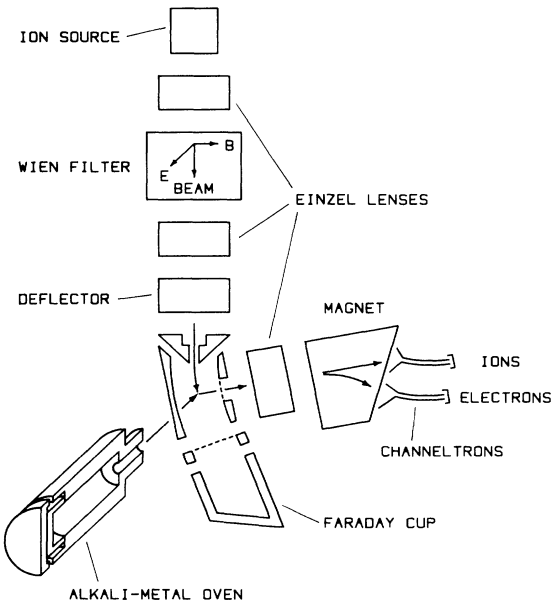

FIG. 2. Schematic diagram of crossed-beam apparatus.

The alkali-metal oven is made of stainless steel and sealed with a removable cap made of Monel alloy. The oven is heated by iron-Constantan thermocouple wire[10] wrapped around the grooved outside surface. The exit cylinder of the oven is densely wrapped with the heating wire so that it can be maintained hotter than the main body of the oven; this prevents clogging of the exit orifice and reduces the dimer fraction in the atomic beam. A thermocouple attached to the oven monitors its temperature and provides the feedback signal to regulate the current to the heating wire in order to maintain the oven at a present temperature. Typical operating temperatures of the oven are 280°C for K and 350°C for Na. The dimer concentration in each case is negligible, which is evidenced by comparing data obtained at different oven temperatures. The oven together with a separate gas nozzle are mounted on a platform whose rotational position is determined by a worm-gear-motor configuration precisely controlled by electronic sensors. The gas nozzle is identical in shape to the oven's exit cylinder and is used to direct a neutral beam of, e.g., Ar or O_2 into the collision region. This design enables one to monitor and calibrate the apparatus, before and during experiments with alkali-metal vapors, using some previously studied reactants such as $H^- + O_2$ (Ref. 9) and $H^- + Ar$.[11] Liquid-nitrogen-cooled surfaces are positioned to trap the undesired alkali-metal vapor.

The full overlap of the ion beam with the target beam is insured since the target beam has approximately twice the diameter of the ion beam. This overlap is confirmed by the fact that a certain voltage change across the analyzer induces a negligible flux change of the product anions and electrons. The target thickness is chosen such that the attenuation of the ion beam is less than 5%, thus assuring that secondary collisions are negligible.

The relative collection efficiencies for product anion and electron detection systems, at a given collision energy, are determined by normalization to the known cross sections, $\sigma_e(E)$ and $\sigma_{CT}(E)$, for $H^- + O_2$.[9] These two cross sections for $H^- + O_2$ are comparable in magnitude over the energy range of interest. The normalization procedure yields energy-dependent transmission functions for the product anion and electron collecting systems. The transmission function for anions is slightly different from that for electrons mainly because of the different effects of the magnetic field. These relative transmission functions are found to deviate from unity by no more than $\pm 10\%$ over the energy range of $5 \leq E \leq 300$ eV. For reasons that will be discussed below, the transmission functions cannot be ascertained by using O_2 as the target gas while the alkali-metal oven is hot. However, the transmission function for electron collection may be confirmed with $H^- + Ar$ (with the argon gas passing through a *U*-shaped liquid-nitrogen-cooled tube) during

experiments involving alkali-metal vapor.

There are two sources of extraneous signals in the experiments. First, as might be expected, some signals will be collected by the electron multipliers even with no target vapor in the collision region. This is primarily due to stray electrons which result from collisions of a fraction of the ion beam with electrostatic lenses and apertures. The effect of these "gas-out" electrons is measured by turning the alkali-metal beam away from the collision region and determining background signals.

The second and more vexing source of extraneous signals is related to the presence of alkali-metal atoms on the surfaces within the collision region. Even with no ion beam in the collision region, some negatively charged particles are observed to desorb from the alkali-coated surface and arrive at the two-particle multipliers. The intensity of these particles increases dramatically as one increases the partial pressure of oxygen or water vapor in the vacuum chamber and, in fact, can easily saturate both particle multipliers. This problem prevents one from using $H^- + O_2$ to calibrate the apparatus during the alkali-metal experiments. These negatively charged particles which come from alkali-coated surfaces include both electrons and anions; their production mechanism remains unexplained at this time. Fortunately, in the present experiment environment, the extraneous signals caused by the alkali-coated surfaces decrease when the temperature of the oven increases; at the appropriate temperature to do the experiments, these extraneous signals are about one-eighth of the authentic signals. The background contribution due to these particles is measured by steering the ion beam away from the collision region and observing the resultant signals present with a zero-intensity negative ion beam.

Data obtained with the apparatus described above is repeatable to within 10%. Using the transmission functions determined with $H^- + O_2$, earlier total cross-section measurements for $D^- + O_2$ (Ref. 9) and $H^- + Ar$ (Ref. 11) can be reproduced with the present apparatus to within the reported experimental uncertainties associated with those results. Combining these facts, we conclude that the systematic error associated with the present apparatus is less than 20%.

B. Differential cross-section apparatus

The differential cross-section measurements were performed on an apparatus which has been described previously[12] with the one exception of the collision chamber. The revised collision chamber can be heated so that alkali metals may be used for gas-phase targets. After several hours, the temperature of the collision chamber is constant to within 1 K and is such that the sodium vapor pressure is about 5×10^{-4} Torr during an experimental run. The use of alkali metals in the collision chamber may lead to substantial contact potentials which limit the accuracy to which the kinetic energy of the negative ion beam may be determined. The resulting uncertainty in the laboratory kinetic energy, as determined by a 127° electrostatic cylindrical velocity selector, is estimated to be about 1.5 eV. A justification for this estimate will be given later. Differential cross-section measurements were limited to laboratory angles larger than 5°.

III. RESULTS AND DISCUSSION

A. Elastic scattering of $H^- + Na$

Some experimental results for the elastic differential cross section for collisions of $H^- + Na$ are shown in Fig. 3. The rainbow maxima are clearly seen at the reduced scattering angle, $E\theta\approx80$ eV deg for the two lower collision energies (8.8 and 11.3 eV) whereas an additional feature has been resolved in the 15.1 eV experiment. The maximum associated with rainbow scattering cannot be seen in 15.1 eV experiment owing to small-angle contamination by the (unscattered) primary ion beam.[12] The calculation shown in Fig. 3(a) is the result of a partial-wave calculation for $\sigma(\theta)$ in which the ground electronic state of NaH^- (Fig. 1) is used to compute the JWKB phase shifts. This calculation of the differential cross section (which has been convoluted) is for a relative collision energy of 8.8 eV.

When presented in reduced coordinates, as in Fig. 3, the calculated cross section depends very little upon the collision energy; a calculation for $E=11.3$ eV is indistinguishable from that for $E=8.8$ eV. This scaling feature allows us to estimate an upper limit for the uncertainty (due to contact potentials) in the collision energy. If

$$\tau_1\equiv E_{1\text{expt}}\theta_1=(E_{1\text{true}}+\delta E)\theta_1$$

and

$$\tau_2\equiv E_{2\text{expt}}\theta_2=(E_{2\text{true}}+\delta E)\theta_2$$

are defined as the experimentally observed rainbow maxi-

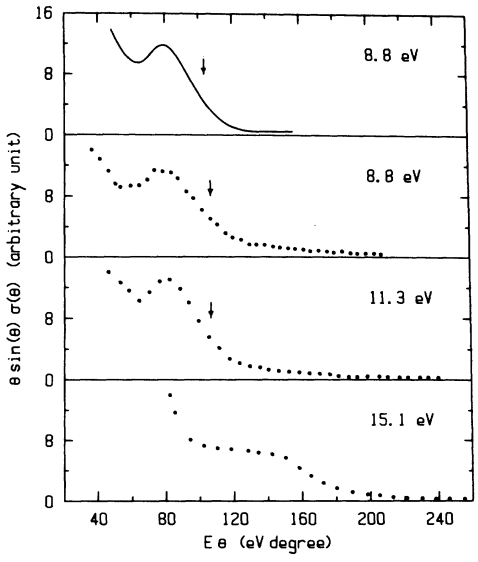

FIG. 3. Reduced elastic differential cross section $[\sigma(\theta)\theta\sin\theta]$ versus reduced angle $(E\theta)$ for $H^- + Na$. (a) Result of JWKB calculation. (b), (c), and (d) experimental measurements. The arrows mark the rainbow angles.

ma for the two different experiments [Figs. 3(b) and 3(c)], then the uncertainty in energy can be estimated as

$$\delta E \simeq \frac{\delta\tau}{\theta_2-\theta_1} ,$$

where $\delta\tau$ is the limiting accuracy for which the observed maxima can be said to be invariant with collision energy. From Figs. 3(b) and 3(c), δE can be estimated to be approximately 1.5 eV. The rainbow angle (corresponding to the scattering angle for which the differential cross section drops to 44% of that at the rainbow maximum) as determined in the experiments is about 106 eV deg (as shown by arrows in Fig. 3), which agrees well with the predicted value of 103 eV deg.[4]

The break which occurs at $E\theta \approx 150$ eV deg in the differential cross section observed in the 15.1 eV experiment [Fig. 3(d)] cannot readily be observed in the lower-energy experiments, presumably due to the rather small signal-to-noise ratios for $E\theta > 120$ eV deg in these experiments.

Sharp depletion of elastic cross sections is typical for slow collisions of anions with atoms[2] and can only be attributed to strong coupling near a curve crossing. The reduced angle of 150 eV deg corresponds to a trajectory with the classical turning point $R_{TP} \approx 2.7a_0$. This strongly suggests that the ground negative-ion potential curve does in fact cross into the neutral continuum around $R=2.7a_0$. Autodetachment due to such a crossing may therefore yield an electron detachment cross section as high as 6 Å^2.

As will be seen, charge transfer is not important at these low collision energies. It is therefore reasonable to expect that the elastic differential cross section (in the rainbow region) is simply determined by the ground electronic state of NaH^-.

B. Charge transfer and electron detachment of $H^-(D^-)$ + Na

The measured cross sections for charge transfer $\sigma_{CT}(E)$ and electron detachment $\sigma_e(E)$ for collisions of H^- with Na are shown in Fig. 4 as functions of relative collision energy. Since the target thickness in our crossed-beam experiments could not be measured accurately, the absolute value of the cross sections reported here were not experimentally determined. We have chosen to normalize $\sigma_{CT}(E)$ to Olson and Liu's calculation[4] at high energy in order to facilitate comparison. As may be seen in Fig. 4, the energy dependence of $\sigma_{CT}(E)$ agrees well with this calculation. However, the measured electron detachment cross sections seriously disagree with their prediction that $\sigma_e/\sigma_{CT} \leq 0.5$. There are several possible reasons for this disagreement; they will be discussed below.

First, it is useful to refer to the potential curves for NaH and NaH^- in Fig. 1. These curves are obtained by means of a cubic-spline fit to the numerical results reported by Olson and Liu.[4] Their calculated asymptotic separation between the $X\,^2\Sigma$ and $X\,^1\Sigma$ states is 0.554 eV, deviating from the electron affinity of hydrogen by 0.20 eV (presumably because the correlation energy between the core and valence electrons was not included for NaH^-, whereas it was for NaH). Therefore, the curves shown in Fig. 1 for the negative ionic states have been shifted down relative to the neutral molecular state to

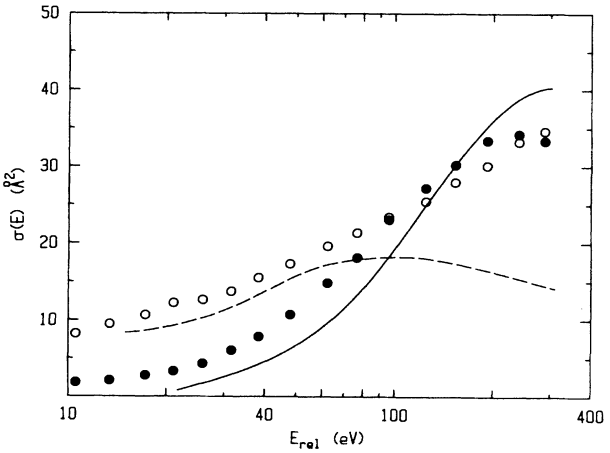

FIG. 4. Measured $\sigma_{CT}(E)$ (solid circles) and $\sigma_e(E)$ (open circles). Solid line is the calculated $\sigma_{CT}(E)$ from Ref. 4 and Eq. (3). Dashed line is the calculation of Eq. (4) plus 6.4 Å^2 (see text).

compensate for this asymptotic error. As may be seen, even with such adjustment, the $X\,^2\Sigma$ state still crosses into the $X\,^1\Sigma$ continuum around $R=2.7a_0$, agreeing with our measurements of the differential elastic cross sections and the calculation by Karo *et al.* The schematic presented in Ref. 4 shows no such crossing although their numerical results plotted in Fig. 1 clearly indicate a crossing. This crossing (which was ignored in Ref. 4) will clearly contribute to $\sigma_e(E)$ with a maximum cross section of about 6 Å^2.

Second, it is useful to review the two-state PSS calculation for the charge-transfer and electron-detachment cross sections as presented in Ref. 4. In this calculation, it is assumed that the electron loss of H^- is due primarily to a long-range coupling between the $X\,^2\Sigma$ and $A\,^2\Sigma$ states. In order to determine a diabatic coupling matrix element between these two states of NaH^-, a point-charge-induced interaction ($\alpha/2R^4$) is assumed for the diabatic curves. By comparing these diabatic curves with the calculated adiabatic $X\,^2\Sigma$ and $A\,^2\Sigma$ curves at large internuclear distance ($R=10$–$20a_0$), the diabatic coupling matrix element is found to be

$$H_{12}(R)=0.0274\exp(-0.171R) . \quad (1)$$

Probability evolution on each channel is then calculated by using a two-state PSS method with straight-line trajectories. In that model, the amplitude for the particles to be in the upper $A\,^2\Sigma$ state is

$$C_2(b,v,x)=(i\hbar v)^{-1}\int_{-\infty}^{x} H_{12}\exp(i\phi)dx' \quad (2)$$

with

$$\phi(b,v,x)=(\hbar v)^{-1}\int_0^x (H_{22}-H_{11})dx'$$

in first-order approximation ($C_1=1$), where H_{11} and H_{22} are the diabatic potential curves, C_1 and C_2 the amplitudes on states $X\,^2\Sigma$ and $A\,^2\Sigma$, b is the impact parameter, v the collision velocity, and x is vt ($t=0$ at the turning point, see Fig. 5).

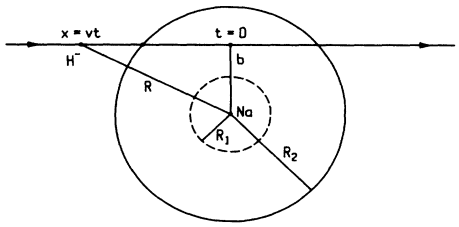

FIG. 5. $H^- + Na$: a straight-line trajectory of H^- in the rest frame of Na. Dashed- and solid-line circles indicate where the $X\,^2\Sigma$ and $A\,^2\Sigma$ states cross into the $X\,^1\Sigma$ continuum, respectively.

For the trajectories, with $b > R_2$ (the internuclear separation at which the $A\,^2\Sigma$ state crosses into the $X\,^1\Sigma$ continuum, viz., $R_2 = 7.4a_0$), the coupling leads only to charge transfer. The resultant charge-transfer cross section is

$$\sigma_{CT}(v) = \int_{R_2}^{\infty} |C_2(b,v,\infty)|^2 2\pi b\, db \ . \tag{3}$$

For $b < R_2$, the $A\,^2\Sigma$ state may yield electron detachment when $R < R_2$. In fact, unit probability was assumed for electron ejection from the $A\,^2\Sigma$ state at this crossing. In other words, the long-range interaction between the target and the incoming projectile ($t < 0$) on a trajectory with $b < R_2$ contributes to the electron-detachment cross section

$$\sigma_e(v) = \int_0^{R_2} |C_2(b,v,-(R_2^2 - b^2)^{1/2})|^2 2\pi b\, db \ . \tag{4}$$

Numerical calculations using (3) and (4) have been performed. Our calculated charge-transfer cross sections duplicate those presented in Ref. 4 to within 5%, yet we get very different results for electron detachment due to the long-range coupling, viz., $\sigma_e(E)$ is found to be larger than $\sigma_{CT}(E)$ for energies below 70 eV or so. These results seem reasonable and they are supported by the following arguments. The higher collision velocity allows charge transfer to occur at larger internuclear distances for the same reason given in Ref. 4 to explain why a lighter alkali metal yields larger cross sections; i.e., the smaller gap between $X\,^2\Sigma$ and $A\,^2\Sigma$ for the lighter alkali metal allows reactions to occur at larger impact parameters. In other words, the effective radius of the long-range coupling shrinks when the impact velocity decreases, or the effective region of the coupling for $b < R_2$ represents a larger fraction of the total inelastic scattering cross section at low energy. Thus, it is understandable that the result of (4) will be larger than that of (3) at low energy.

It should be mentioned that the contribution to σ_{CT} for outgoing trajectories (i.e., $t > 0$) on a trajectory with $b < R_2$ is not included in (3). The magnitude of this contribution is uncertain due to a lack of information about the coupling for $R < R_2$.

Let us now consider the additional detachment due to the crossing of the $X\,^2\Sigma$ and $X\,^1\Sigma$ states at $R_1 = 2.7a_0$. Since the survival probabilities of H^- are large, we can, to first order, treat the various electron-loss channels independently. Clearly the $X\,^2\Sigma$-$X\,^1\Sigma$ crossing contributes to electron detachment a maximum of πR_1^2. This, combined with that predicted by (4), can well account for the measured electron-detachment cross sections at low energy, as shown by the dashed line in Fig. 4. The gap between the dashed line and the measured electron-detachment cross sections shows energy dependence similar to the charge-transfer cross sections. This strong energy dependence suggests that there exists another electron-loss channel that is near resonant in nature.[13]

The exit channels for electron loss discussed so far include only $H + Na^-$ and $H + Na + e$. The energy-loss spectra of neutral H for collisions of $H^- + Na$, as measured by Tuan and Esaulov,[6] indicate that the Na^{-*} shape resonance[14,15] plays a role comparable to that for charge transfer to Na^-. Of course, Na^{-*} will autodetach and contribute to our electron-detachment measurements. To the best of our knowledge, no theoretical prediction or explanation exists to account for a substantial production of Na^{-*} in slow collisions of $H^- + Na$.

In what has been presented, any coupling between $X\,^2\Sigma$ and states other than $X\,^1\Sigma$ states for $R < R_2$ has been ignored. Although the coupling between $X\,^2\Sigma$ and $X\,^1\Sigma$ might be negligible for $R > R_1$, the coupling between $X\,^2\Sigma$ and $A\,^2\Sigma$ will be much larger because the electron wave in the $A\,^2\Sigma$ state is localized. The $A\,^2\Sigma$ state in that region is mainly $H^- + Na(3P)$ in a diabatic representation for the system NaH^-. The collisional transition from $H^- + Na(3S)$ to $H^- + Na(3P)$ can be easily understood with the large polarizability of Na in mind. When H^- approaches Na, the electron wave around Na becomes deformed, i.e., a p-wave component appears. The system in the $A\,^2\Sigma$ state cannot autodetach easily because the p-wave centrifugal barrier will trap the extra electron temporarily. Thus, the two-state PSS method with straight-line trajectories may still be a good approximation to describe transitions between $X\,^2\Sigma$ and $A\,^2\Sigma$ for $R < R_2$. The calculation will be straightforward as long as a reasonable coupling term is provided. A transition to the $A\,^2\Sigma$ state in the region $R < R_2$ may yield to $B\,^2\Sigma$ or $H + Na^{-*}$ states due to the expected strong coupling near the avoided crossing between $A\,^2\Sigma$ and $B\,^2\Sigma$.

In summary, for charge transfer in slow collisions of H^- with Na, the mechanism is simply the long-range coupling between $X\,^2\Sigma$ and $A\,^2\Sigma$; a previous calculation[4] agrees well with our measurements. For the electron detachment, on the other hand, there are several responsible mechanisms: (1) autodetachment due to the crossing of $X\,^2\Sigma$ into $X\,^1\Sigma$; (2) charge transfer to $A\,^2\Sigma$ for $b < R_2$ and $t < 0$ and, thereafter, detachment due to the crossing of $A\,^2\Sigma$ into $X\,^1\Sigma$; and (3) charge transfer to $A\,^2\Sigma$ in $R < R_2$ and thereafter transition to $B\,^2\Sigma$ or $H + Na^{-*}$ shape resonance state due to the avoided crossing between $A\,^2\Sigma$ and $B\,^2\Sigma$.

The measurements of σ_{CT} and σ_e for collisions of D^- with Na (and $H^- + Na$) are shown in Fig. 6 as functions of E/M. As may be seen, both σ_{CT} and σ_e display velocity dependent isotope effects which are consistent with the theories discussed above; the two-state PSS method with straight-line trajectories inherently contains a velocity dependent isotope effect for H^- and D^-.

The experimental ratios σ_{CT}/σ_e for $H^-(D^-) + Na$ are

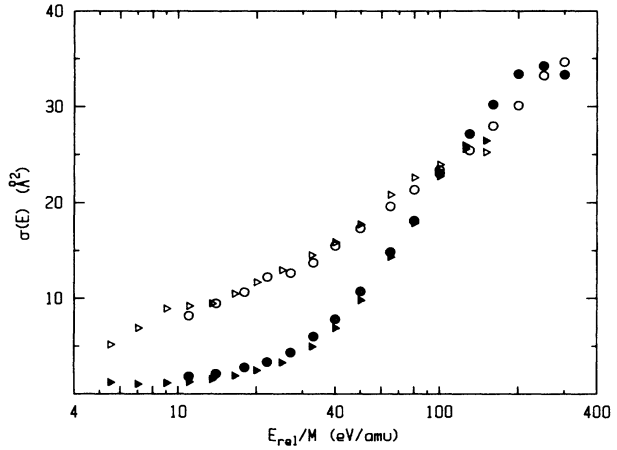

FIG. 6. Measured σ_{CT} (solid symbols) and σ_e (open symbols) for $H^- + Na$ (circles) and $D^- + Na$ (triangles) versus E_{rel}/M, where E_{rel} is the relative collision energy and M the reduced mass of the projectiles.

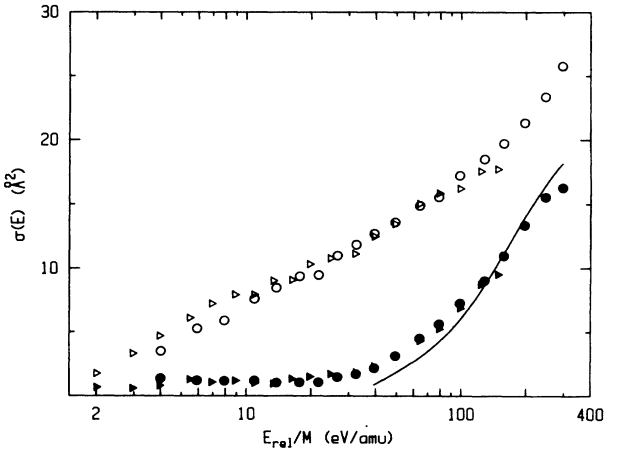

FIG. 8. Measured σ_{CT} (solid symbols) and σ_e (open symbols) for $H^- + K$ (circles) and $D^- + K$ (triangles) versus E_{rel}/M. Solid line is the calculated σ_{CT} from Ref. 4.

presented in Fig. 7. Also shown in Fig. 7 are the ratios for $H^- + Na$ estimated by Tuan and Esaulov[6] based on their measurements of the differential energy-loss spectra of the scattered H atoms. Their results are in good agreement with the present measurements at the higher collision energies.

C. Charge transfer and electron detachment of $H^-(D^-) + K$

The measurements of σ_{CT} and σ_e for collisions of H^- and D^- with K are shown in Fig. 8 as functions of E/M. The experimental ratios σ_{CT}/σ_e for $H^-(D^-) + K$ are also shown in Fig. 9. As for Na, we have chosen to normalize the measured σ_{CT} for $H^- + K$ to Olson and Liu's calculation at high energy. As may be seen in the figure, the general structure of σ_{CT} and σ_e for K are very similar to those for Na. This feature suggests that the electron-loss mechanisms are the same for these two targets. The threshold of σ_{CT} for K is higher than that for Na and the overall cross sections for K are smaller than those for Na. These differences are due to the fact that K has smaller electron affinity and larger dipole polarizability, and consequently a larger energy gap between the $X\,^2\Sigma$ and $A\,^2\Sigma$ states of KH^-.[4]

IV. SUMMARY

Both charge transfer and electron detachment are significant electron-loss mechanisms in slow collisions of H^- and D^- with Na and K. Both processes exhibit a velocity dependent isotope effect for H^- and D^-. $\sigma_{CT}(E)$ displays a strong energy dependence and high energetic thresholds

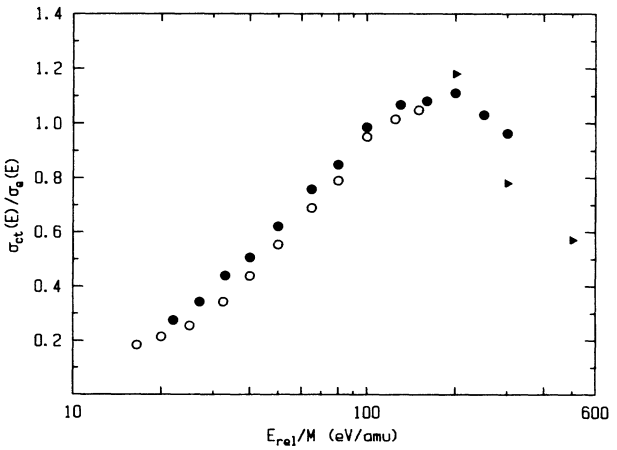

FIG. 7. Measured ratios σ_{CT}/σ_e for $H^- + Na$ (solid circles) and $D^- + Na$ (open circles) versus E_{rel}/M. Solid triangles are the ratios for $H^- + Na$ taken from Ref. 6.

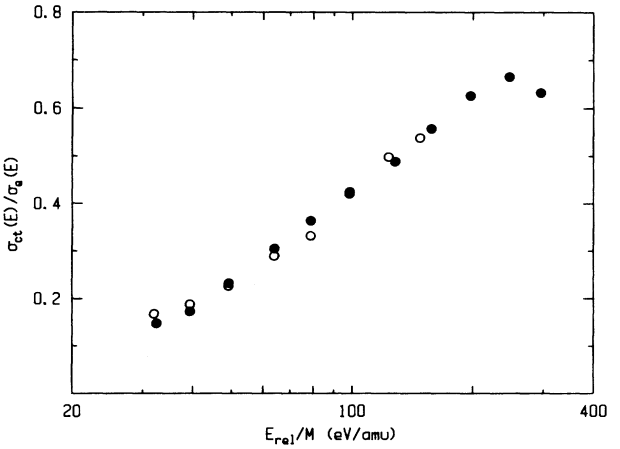

FIG. 9. Measured ratios σ_{CT}/σ_e for $H^- + K$ (solid circles) and $D^- + K$ (open circles) versus E_{rel}/M.

(about 20 eV for $H^- + Na$ and 40 eV for $H^- + K$), while $\sigma_e(E)$ displays weaker energy dependence and apparent zero-energy thresholds. The elastic differential cross sections for $H^- + Na$ exhibit rainbow maxima and indicate a curve crossing; these observations are consistent with the molecular state calculations.[3,4]

Although there have been several successful models to describe the electron detachment for collisions of H^- with rare gases,[2,8,13,16] a new model or a combination of models is required to completely describe the electron-loss mechanisms for collisions of H^- with alkali-metal atoms. In particular, it will be very interesting to understand the role of the Na^{-*} shape resonance state in the collisional dynamics for these reactants.

ACKNOWLEDGMENTS

The authors wish to thank R. V. Z. Meredith for checking the numerical integrals of (3) and (4). This work was supported in part by the U.S. Department of Energy, Office of Basic Energy Sciences.

[1]J. R. Hiskes, A. M. Karo, and M. A. Gardner, J. Appl. Phys. **47**, 3888 (1976).
[2]R. L. Champion, Adv. Electron. Electron Phys. **58**, 143 (1982).
[3]A. M. Karo, M. A. Gardner, and J. R. Hiskes, J. Chem. Phys. **68**, 1942 (1978).
[4]R. E. Olson and B. Liu, J. Chem. Phys. **73**, 2817 (1980).
[5]F. W. Meyer, J. Phys. B **13**, 3823 (1980).
[6]V. N. Tuan and V. A. Esaulov, Phys. Rev. A **32**, 883 (1985).
[7]A. S. Schlachter, K. R. Stalder, and J. W. Stearns, Phys. Rev. A **22**, 2494 (1980).
[8]S. K. Lam, J. B. Delos, R. L. Champion, and L. D. Doverspike, Phys. Rev. A **9**, 1828 (1974).
[9]M. S. Huq, L. D. Doverspike, and R. L. Champion, Phys. Rev. A **27**, 785 (1982).
[10]The heating wire used for the alkali oven is Omegaclad iron-Constantan thermocouple wire (304-J-MO-062) manufactured by Omega Engineering, Inc., which is metal-sheathed and contains magnesium oxide insulation.
[11]R. L. Champion, L. D. Doverspike, and S. K. Lam, Phys. Rev. A **13**, 617 (1976).
[12]R. L. Champion, L. D. Doverspike, W. G. Rich, and S. M. Bobbio, Phys. Rev. A **2**, 2327 (1970). This paper contains a discussion of rainbow scattering. Also, see R. B. Bernstein, in *Advances in Chemical Physics,* edited by J. Ross (Wiley, New York, 1966), Vol. X, p. 75.
[13]J. P. Gauyacq, J. Phys. B **12**, L387 (1979).
[14]A. R. Johnston and P. D. Burrow, J. Phys. B **15**, L745 (1982).
[15]A. L. Sinfailam and R. K. Nesbet, Phys. Rev. A **7**, 1987 (1973).
[16]J. B. Delos, Rev. Mod. Phys. **53**, 287 (1981).